

Adsorption State and Molecular Orientation of Ammonia on ZnO(10 $\bar{1}$ 0) Studied by Photoelectron Spectroscopy and near-Edge X-ray Absorption Fine Structure Spectroscopy

K. Ozawa,^{*,†} T. Hasegawa,[†] K. Edamoto,[†] K. Takahashi,[‡] and M. Kamada^{‡,§}

Department of Chemistry and Materials Science, Tokyo Institute of Technology, Ookayama, Meguro-ku, Tokyo 152-0033, Japan, and Institute for Molecular Science, Myodaiji, Okazaki 444-8585, Japan

Received: March 1, 2002; In Final Form: June 4, 2002

The adsorption state of ammonia (NH₃) on the ZnO(10 $\bar{1}$ 0) surface has been investigated using photoelectron spectroscopy (PES) and near-edge X-ray absorption fine structure (NEXAFS) spectroscopy. The core-level and valence-band PES measurements reveal that ammonia adsorbs molecularly via its N atom on ZnO(10 $\bar{1}$ 0) and that no dissociated species are formed at room temperature. The orientation of adsorbed NH₃ is investigated by the polarization-dependent N K-edge NEXAFS measurements, and it is found that the C_{3v} molecular axis of NH₃ is inclined in the [000 $\bar{1}$] direction with the tilt angle of 33°–41° from the surface normal.

I. Introduction

Ammonia synthesis has been one of the most important subjects in the chemical industry for nearly a century since the Haber–Bosch process was developed. In the process, iron oxide admixed with a small amount of alkali-metal and/or alkaline-earth-metal oxides is used to facilitate the synthetic reaction.¹ In addition, ammonia is an important reactant for nitric acid synthesis in the Ostwald process, which involves the catalytic oxidation of ammonia in the first step to produce nitric oxides. For this reaction, platinum–rhodium alloys are commonly used as catalysts, but possible usefulness of metal oxides is discussed in a recent literature.² Thus, interaction of ammonia with metal-oxide surfaces is of great importance from the viewpoint of industrial chemistry.

In a generally accepted model for ammonia adsorption on the metal-oxide surfaces, an ammonia molecule acts as a strong Lewis base and adsorbs preferentially at Lewis acid sites, i.e., metal-ion sites, through the σ -type interaction between the N-localized 3a₁ molecular orbital (MO) and the unoccupied orbitals of the metal ions. The adsorption mechanism of this type is predicted theoretically^{3–5} and is actually observed experimentally^{6–9} for many NH₃/metal-oxide systems, where ammonia is proved to be bound to the surface metal ions via its N atom.

Interaction of ammonia with the ZnO surfaces can be viewed as a prototype of the NH₃/metal-oxide systems, and thus it has been studied both experimentally and theoretically. Lin et al. have investigated the adsorption state of ammonia on the Zn-terminated ZnO(0001) surface utilizing photoelectron spectroscopy (PES) and scattered-wave (SW) X α MO calculations¹⁰ and have found that ammonia adsorbs on the surface through the orbital hybridization between the NH₃ 3a₁ and Zn 4sp orbitals. It is also found that, aside from physisorbed and molecularly chemisorbed NH₃, partially decomposed species are formed with a certain amount on ZnO(0001) at 130 K.¹⁰

Regarding the nonpolar ZnO(10 $\bar{1}$ 0) surface, which is composed of equal numbers of the Zn and O atoms, it is suggested from the PES and constant-initial-state spectroscopy (CIS) measurements that ammonia adsorbs on the surface Zn atoms in the molecular form.^{11,12} A recent density functional (DF) cluster calculation by Casarin et al. has indicated that, unlike the NH₃/ZnO(0001) system, molecular adsorption is favored on ZnO(10 $\bar{1}$ 0).⁵ However, a detailed picture of ammonia adsorption on ZnO(10 $\bar{1}$ 0) has not been clarified experimentally so far.

The purpose of the present study is to reveal the adsorption state of NH₃ on ZnO(10 $\bar{1}$ 0) by the use of PES and the near-edge X-ray fine structure (NEXAFS) spectroscopy. It is found that ammonia adsorbs molecularly through the interaction between the NH₃ 3a₁ orbital and the substrate's orbitals and that no dissociated species are formed at room temperature. Polarization-dependent measurements of the NEXAFS spectrum were carried out to estimate the orientation of adsorbed NH₃ on ZnO(10 $\bar{1}$ 0). The NEXAFS technique is a well-established method to determine the orientation of adsorbed species.^{13–16} However, this technique has not been applied so far to adsorbed ammonia, partly because the NEXAFS spectra of adsorbed NH₃ show only broad resonance features with a poor polarization dependence compared with the adsorbates with π conjugated systems.^{17–19} Regarding adsorbed ammonia, therefore, electron stimulated desorption ion angular distribution (ESDIAD),^{20,21} X-ray photoelectron diffraction (XPD),²² and X-ray emission spectroscopy (XES)¹⁹ have been used to investigate the molecular orientation on the surfaces. The present study demonstrates that the polarization-dependent NEXAFS measurements combined with curve-fitting analysis are also useful to determine the orientation of adsorbed NH₃.

II. Experimental Section

Instrumentation. The PES measurements utilizing He I resonance line and Al K α radiation were carried out in the ultrahigh vacuum (UHV) system equipped with a Mg/Al dual anode X-ray source, a He I discharge lamp, a 180° spherical-sector-type electron-energy analyzer and low-energy electron diffraction (LEED) optics. Directions of the incidence light of X-ray and He I radiation were fixed at 135° and 45° from the analyzer axis, respectively. The base pressure of the system was $\sim 5 \times 10^{-10}$ Torr. For the X-ray PES measurements, the ZnO-

* Corresponding author. Fax: +81 3 5734 2655. E-mail: kozawa@chem.titech.ac.jp.

[†] Tokyo Institute of Technology.

[‡] Institute for Molecular Science.

[§] Present address; Synchrotron Light Application Research Center, Saga University, Honjyou 1, Saga 840-9502, Japan.

(10 $\bar{1}$ 0) surface was oriented so that the detection angle of photoelectrons was 50°–60° from the surface normal. The binding energy was referenced to the position of the O 1s peak at 530.5 eV for core-level photoemission (PE) spectra.²³ For the valence-band PES measurements, the photoelectrons emitted to the normal direction were collected. The binding energy of the valence-band PE spectra was referenced to zero at the Fermi level (E_F), which was derived from the Fermi edge in the spectra from the tantalum sample holder.

The PES and NEXAFS measurements utilizing synchrotron radiation were performed at beam line 2B1 of the Ultraviolet Synchrotron Orbital Radiation (UVSOR) Facility, Institute for Molecular Science. Synchrotron radiation was monochromatized by a grasshopper monochromator (Baker Manufacturing). The UHV chamber at the end of the beam line was equipped with a double-pass cylindrical mirror analyzer (CMA), LEED optics and a quadrupole mass spectrometer. The CMA axis was fixed at 80° from the incidence direction of the light. The base pressure in the UHV chamber was lower than 2×10^{-10} Torr. For the NEXAFS measurements, the azimuthal orientation of the ZnO(10 $\bar{1}$ 0) surface was chosen so that the incidence plane of the light was parallel to the [000 $\bar{1}$] azimuth. The light was linearly polarized in the incidence plane. By rotating the sample, the incidence angle of the light (θ_i) relative to the surface normal was changed so that the ratio between the parallel and perpendicular components of the electric vector E of the light was varied. The N K-edge NEXAFS data were recorded in the N KLL Auger electron yield mode with a constant final state energy of 375 eV. The photon energy was calibrated using the absorption feature at 284.5 eV in the photocurrent, which is associated with the π^* resonance of highly oriented pyrolytic graphite (HOPG) formed on the gold mesh as a contaminant.²⁴ The accuracy of the photon energy is ± 1 eV.

Sample Preparation. The ZnO single crystal ($10 \times 10 \times 1$ mm³; Mateck) was fixed on the Ta holder and was mounted on a rotatable manipulator so that the incidence angle of the light and the detection angle of the photoelectrons were able to be varied. The (10 $\bar{1}$ 0) surface was cleaned in situ as follows: The cycles of Ar⁺ sputtering (1.6 kV, 2–3 μ A) and annealing at 1050 K were carried out for several times in UHV until the surface contamination was not detected in the core-level PE spectra. The sample was then annealed at 700 K in O₂ atmosphere (4×10^{-6} Torr) for 10–15 min and cooled to 500 K before O₂ was pumped out. After cooling to room temperature, the sample was annealed at 600 K for 10 min. The clean ZnO(10 $\bar{1}$ 0) surface thus prepared showed a (1 \times 1) LEED pattern. For ammonia adsorption, research-grade ammonia gas (99.99%, Takachiho) was introduced into the chamber through a variable leak valve. The sample was kept at room temperature during exposure. Sample temperature was monitored by a chromel–alumel thermocouple, which was spot-welded to the sample holder and was in direct contact with the rear of the sample crystal.

Analysis of NEXAFS Spectra. The N K-edge NEXAFS spectra presented in the present paper were doubly normalized by dividing the spectra of the NH₃-covered surface by the photon flux estimated from the photocurrent of a gold mesh at the entrance of the UHV chamber and by the spectrum of the clean surface, which was also normalized by the photon flux, so that the NH₃-induced peaks were extracted. However, these NH₃-induced peaks were weak and broad compared with the resonances of the adsorbates with π -conjugated systems, and this made the analysis of the θ_i -dependent change in the peak intensity difficult. Thus, to clarify the individual peak and the

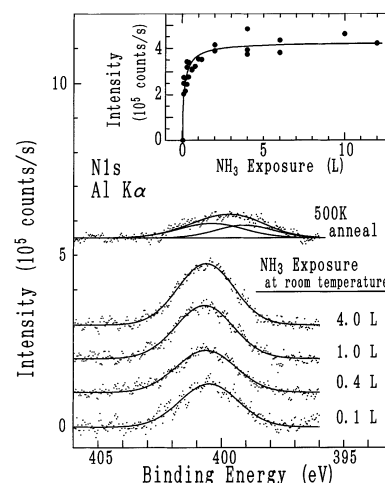


Figure 1. Change in the N 1s core-level PE spectrum of the ZnO(10 $\bar{1}$ 0) surface exposed to ammonia at room temperature. The uppermost spectrum is obtained from the 4-L NH₃-exposed surface which is annealed at 500 K for 2 min. A polynomial-type background is subtracted from each raw spectrum. The solid lines are the best fitted results by the Gaussian functions. The inset shows the change in the integrated intensity of the N 1s peak as a function of exposure at room temperature. Saturation is reached at ~ 2 L, which corresponds to the NH₃ coverage of $\Theta \approx 0.5$.

θ_i -dependent change in the intensity, the NEXAFS spectra were decomposed by curve fitting using Gaussian functions for the peaks and an error function for the continuum step.²⁵

The deconvolution procedure of the NEXAFS spectra was as follows: First, each spectrum was fitted by the Gaussian functions and the error function under the condition that parameters associated with the position, the width and the amplitude of the Gaussian and error functions were allowed to vary freely. In the second step, since the parameters associated with the position and the width should not depend largely on the experimental geometry, these were fixed at the average of the values obtained from the spectra at different θ_i , and the amplitudes of each peak and the continuum step were optimized by the fitting. Finally, all the parameters were again adjusted simultaneously, but the positions and the widths were fixed at the average values if the optimum values differed significantly from the average values.

III. Results

Adsorption State of NH₃. Figure 1 shows the change in the N 1s core-level PE spectrum of the NH₃-dosed ZnO(10 $\bar{1}$ 0) surface at room temperature as a function of NH₃ exposure. The background, which is approximated by a polynomial function, is subtracted from each raw spectrum. As the ZnO(10 $\bar{1}$ 0) surface is exposed to NH₃, a peak with a symmetric line shape appears at 400.5 eV at 0.1 L ($1 \text{ L} = 1 \times 10^{-6}$ Torr s). The peak intensity increases with increasing exposure and saturates at ~ 2 L, as shown in the inset of Figure 1, indicating that adsorption saturates at ~ 2 L at room temperature. The peak position and the line shape do not exhibit substantial changes by the increase in the NH₃ exposure, and each N 1s peak is reproduced by a single Gaussian function (solid line). However, because the NH₃-exposed surface is annealed, the profile of the N 1s peak becomes asymmetric due to the development of a new component at the low binding energy side. The uppermost spectrum in Figure 1 shows a spectrum of the 4-L NH₃-exposed surface subject to annealing at 500 K for 2 min. In this case, the observed peak is reproduced by two Gaussian functions; one lies at 400.5 eV, which coincides with the peak from the

surface exposed to NH_3 at room temperature, and the other at 399.0 eV, which is the anneal-induced peak. It is known that the N 1s peak from molecularly adsorbed ammonia on metal and semiconductor surfaces appears at 400–401 eV, whereas the partially decomposed species, i.e., NH_x ($x = 1, 2$), give the N 1s peak at 398–399.4 eV.²⁶ Thus, the peak at 400.5 eV is well associated with the molecularly adsorbed ammonia, and the decomposed NH_x species is responsible for the 399.0-eV peak. These observations indicate that ammonia adsorbs molecularly on the $\text{ZnO}(10\bar{1}0)$ surface at room temperature, and adsorbed NH_3 undergoes the decomposition reaction upon annealing the surface. Our recent PES study have revealed that dissociation of adsorbed NH_3 starts already at the anneal temperature of 350 K and that the dissociation reaction competes with the desorption reaction.²⁷ It is also found that the adsorbed species of both molecularly adsorbed and partially decomposed ammonia are eliminated from the surface up to 650 K.²⁷

For the $\text{NH}_3/\text{ZnO}(10\bar{1}0)$ system, no NH_3 -adsorption induced LEED pattern is observed, and thus, information on the ammonia coverage cannot be obtained from the LEED measurements. We estimate the ammonia coverage Θ using the intensities of the N 1s peak from the NH_3 -adsorbed surface ($I_{\text{N}1\text{s}}$) and the O 1s peak from the clean surface ($I_{\text{O}1\text{s}}$) utilizing the following equation:²⁸

$$\Theta = \frac{N_{\text{am}}}{N_{\text{O}}} = \frac{I_{\text{N}1\text{s}} \sigma_{\text{O}1\text{s}}}{I_{\text{O}1\text{s}} \sigma_{\text{N}1\text{s}}} \frac{1 + \exp\{-d_1/\lambda_{\text{O}1\text{s}} \cos \theta_d\}}{1 - \exp\{-(d_1 + d_2)/\lambda_{\text{O}1\text{s}} \cos \theta_d\}}. \quad (1)$$

N_{am} is the number of adsorbed NH_3 per cm^2 , and N_{O} is the atomic density of O in the first layer of the (1×1) substrate surface, i.e., $N_{\text{O}} = 5.90 \times 10^{14}$ atoms/ cm^2 . σ is the photoionization cross section of the core levels. The cross sections of the N 1s and O 1s core-level excitations by Al K α radiation are 0.024 and 0.040 Mb, respectively.²⁹ d_1 and d_2 are the layer spacings between the neighboring $\text{ZnO}(10\bar{1}0)$ planes along the $[10\bar{1}0]$ direction: d_1 corresponds to the distance between the first and second, third and fourth, etc., layers (0.939 Å), and d_2 is the distance between the second and third, fourth and fifth, etc., layers (1.878 Å), if the unrelaxed surface is assumed. $\lambda_{\text{O}1\text{s}}$ is the inelastic mean free path of the O 1s photoelectrons in the ZnO crystal and has been estimated to be 16 Å.³⁰ θ_d is the detection angle of the photoelectron measured from the surface normal direction, and the core-level PE spectra used for the coverage estimation were taken at $\theta_d = 52^\circ$. The intensity ratio $I_{\text{N}1\text{s}}/I_{\text{O}1\text{s}}$ was determined to be 1.64×10^{-2} . Using all these values, we obtain the ammonia coverage of $\Theta = 0.57$. Similarly, $\Theta = 0.52$ is obtained from the intensity ratio of the N 1s peak to the Zn $2p_{3/2}$ peak.³¹ Thus, the saturation coverage is 0.5 at the lowest estimate.

Figure 2 shows the valence-band spectra of the clean and NH_3 -saturated $\text{ZnO}(10\bar{1}0)$ surfaces. The photon energy used was $h\nu = 21.2$ and 130 eV. The spectra of the clean surface (curves a and c) show peaks at 4.0, 7.5 and 10.6 eV, which are associated with the O 2p states, the Zn 4s–O 2p hybrid states and the Zn 3d states, respectively.³² As the surface is covered with the saturation amount of NH_3 , the Zn 3d peak intensity decreases substantially, and the 4.0-eV peak shifts to the higher binding energy side by ~ 0.7 eV (curve b). Since the O 2p band includes the emission from the O 2p dangling bond states on the surface O atoms,³² we attribute the NH_3 -adsorption induced shift of the 4.0-eV peak to the shift of the O 2p dangling bond states. The same trend is observed in the spectrum taken at $h\nu = 130$ eV (curve d), and the difference spectrum (curve e; the spectrum of the NH_3 -saturated surface minus that of the

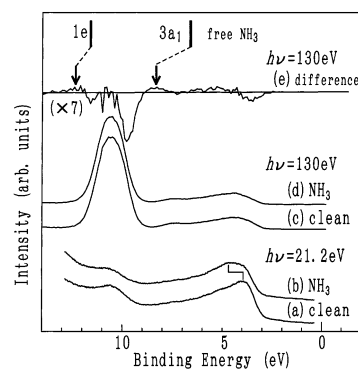


Figure 2. Valence-band spectra of the clean and NH_3 -saturated $\text{ZnO}(10\bar{1}0)$ surfaces taken at room temperature. The uppermost spectrum (curve e) is a difference spectrum produced by curve d minus curve c after normalizing the Zn 3d peak intensity at 10.6 eV. The positions of the $3a_1$ and $1e$ MO's of free NH_3 are indicated by bars.

clean surface after normalizing the Zn 3d peak intensity at 10.6 eV) allows us to see the change of the O 2p peak more clearly. A slight dip and a hump are seen at 3.6 and 5–6 eV, respectively. This can be attributed to the shift of the O 2p dangling bond states to the higher binding energy side by NH_3 adsorption. Another prominent features are dips at the both sides of the Zn 3d peak at 10.6 eV. This means that adsorption induces the narrowing of the observed Zn 3d band. A similar effect is also observed for the $\text{CO}/\text{ZnO}(10\bar{1}0)$ system and is interpreted to be due to the modification of the Zn 3d surface state.¹¹

In the difference spectrum, two more humps are observed at 8.3 and 12.3 eV (indicated by arrows). Adsorbed ammonia in the molecular form on metal surfaces is reported to give the $3a_1$ and $1e$ peaks at 6.7–7.7 and 11–12 eV, respectively.⁶ On the TiO_2 surfaces, the $3a_1$ and $1e$ peaks from NH_3 are found at 6.7–7.4 and 11.4–11.8 eV, respectively.^{6,7} These values are in good agreement with the energies of 8.3 and 12.3 eV for the observed humps in the difference spectrum. Thus, these peaks are ascribed to the emissions from the $3a_1$ and $1e$ MO's of adsorbed NH_3 . This result further supports the conclusion drawn from the core-level PES measurements that ammonia adsorbs molecularly on $\text{ZnO}(10\bar{1}0)$ at room temperature.

In Figure 2, the positions of the $3a_1$ and $1e$ states of free NH_3 are indicated by vertical bars [the ionization energies of the $3a_1$ and $1e$ states are 10.85 and 15.8 eV, respectively,³³ and the work function of the NH_3 -saturated $\text{ZnO}(10\bar{1}0)$ surface is estimated to be 4.2 eV in the present study]. Compared with the energy positions of MO's in free NH_3 , both the $3a_1$ and $1e$ peaks from adsorbed NH_3 on $\text{ZnO}(10\bar{1}0)$ are shifted to the higher binding energy side, meaning that these states are stabilized through the interaction with the substrate surface. However, the shift is larger for the $3a_1$ state (1.65 eV) than the $1e$ state (0.7 eV), and thus the $3a_1$ – $1e$ splitting is diminished from 4.95 eV of the free NH_3 value to 4.0 eV. These results indicate that the relative contribution of the $3a_1$ orbital to the bonding interaction with the surface is larger than the $1e$ orbital. Since the $3a_1$ orbital is an N-localized lone pair orbital, mainly composed of the N $2p_z$ orbital (the z axis is chosen along the C_{3v} axis of NH_3), relatively large stabilization of the $3a_1$ state suggests that NH_3 adsorbs on $\text{ZnO}(10\bar{1}0)$ via its N atom.

Summarizing the adsorption state of ammonia on $\text{ZnO}(10\bar{1}0)$, the core-level and valence-band PES measurements reveal that ammonia adsorbs molecularly and no dissociated species are formed at room temperature. The N-localized $3a_1$ orbital mainly contributes to the chemical bond between NH_3 and the surface, i.e., NH_3 is bound to the $\text{ZnO}(10\bar{1}0)$ surface via its N atom.

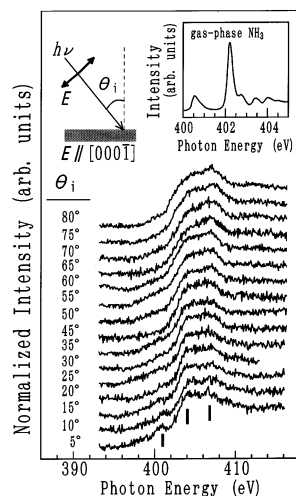


Figure 3. The N K-edge NEXAFS spectra of the NH₃-saturated ZnO(10 $\bar{1}$ 0) surface at various incidence angle θ_i of the light. The incidence plane of the linearly polarized light is parallel to the [000 $\bar{1}$] azimuth. The spectra are normalized by the height of the continuum step. The NEXAFS spectrum of gaseous NH₃ is shown in the inset.³⁴

Orientation of NH₃. Figure 3 shows a series of the N K-edge NEXAFS spectra of the NH₃-saturated ZnO(10 $\bar{1}$ 0) surface as a function of the incidence angle of the light θ_i relative to the surface normal. The NEXAFS spectrum of gaseous NH₃ is also shown in the inset of Figure 3.³⁴ The first resonance feature of free NH₃ is observed at 400.66 eV and is associated with the excitation of the N 1s electron to the lowest unoccupied molecular orbital (LUMO) of NH₃ (4a₁).³⁴ The most pronounced peak at 402.33 eV is related to the N 1s \rightarrow NH₃ 2e excitation state, and three weak features between 402.8 and 404.2 eV are ascribed to the transition to the N 3p, 4s, and 4p orbitals.³⁴ The NEXAFS spectra for NH₃/ZnO(10 $\bar{1}$ 0) do not have such sharp resonances as those of free NH₃, partly because of the formation of the hybrid states between the MO's of NH₃ and the conduction bands of the substrate surface, as discussed below, as well as the lower experimental resolution in the present study. However, at least three resonances are observed at \sim 401, 404, and 407 eV (indicated by bars in the bottom spectrum). A similar three-resonance structure has been also found in the N K-edge NEXAFS spectra for NH₃/Ni(110) by Jaeger et al.¹⁸ and for NH₃/Cu(110) by Hasselström et al.¹⁹ Of the three, two low-excitation-energy resonances are attributed to the transitions from the N 1s core level to the NH₃ 4a₁ and 2e states, and the highest-excitation-energy feature, which is intense and broad compared with the other two, is related to the N 3p and 4sp orbitals hybridized with the substrate orbitals.¹⁹ On the bases of their assignments, we interpret the features at 401 and 404 eV in the present system as the excitations of the N 1s electron to the NH₃ 4a₁ and 2e states, respectively, and the 407-eV peak as the excitation to the hybrid state formed through orbital hybridization between the N 3p and 4sp states and the conduction band of the ZnO surface (we refer to this states as high-lying hybrid states, hereafter). Adsorption-induced orbital hybridization between NH₃ and ZnO(10 $\bar{1}$ 0) should result in the change in the transition probability of the N 1s electrons to the unoccupied hybrid states because of the lowered symmetry of the NH₃ MO's. Such an effect should be significant for the spatially extended N 3p and 4sp orbital, which are responsible for the resonance at 407 eV. This could be the reason the intensity of the high-lying hybrid peak at 407 eV is comparable to that of the 2e peak, although only weak peaks are observed

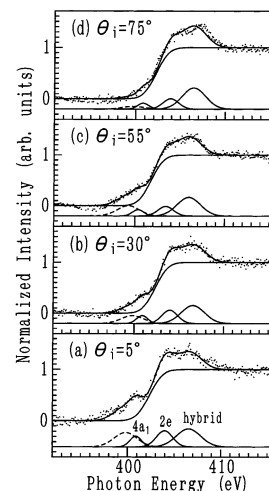


Figure 4. A selected set of the results by curve fitting analysis for the NEXAFS spectra. Four Gaussian functions for the resonance features and an error function for the continuum step are assumed.

in the energy region higher than the pronounced 2e peak for the NEXAFS spectrum of free NH₃ (the inset of Figure 1),

Figure 3 shows that the observed peaks at 401, 404 and 407 eV exhibit a rather weak, but an obvious polarization dependence; the 401-eV feature is observed as a peak at $\theta_i = 5^\circ$ but becomes ambiguous at $\theta_i \geq 20^\circ$, and the 407-eV peak becomes intense compared with the peak at 402 eV with increasing θ_i . To quantify the polarization dependence of these peaks, the NEXAFS spectra were decomposed by curve fitting using Gaussian functions for the peaks and an error function for the continuum step.²⁵ A selected set of the results is shown in Figure 4. Apart from the peaks at 401, 404 and 407 eV, which are related to the 4a₁, 2e and high-lying hybrid states, respectively, another peak (shown by dashed line) is requisite in order to reproduce the low-energy tail structure at \sim 400 eV. Jaeger et al. have observed a similar low energy structure at \sim 398 eV for the NH₃/Ni(110) system and have related it with dissociated ammonia.¹⁸ The NEXAFS spectra for NH₃/Cu(110) also exhibit a weak hump at \sim 400 eV,¹⁹ and the structure is associated with the states formed between the low-lying MO's of NH₃ such as the 3a₁ and 4a₁ orbitals and the Cu 3d orbitals. On the ZnO(10 $\bar{1}$ 0) surface, since ammonia adsorbs molecularly, the possible contribution from the NH_x species can be ruled out. Thus, we tentatively associate this feature to the hybridized states as a result of the NH₃-ZnO interaction, i.e., the antibonding state formed between the occupied 3a₁ orbital of NH₃ and the substrate's orbitals and/or the bonding states between the unoccupied 4a₁, 2e, etc., orbitals and the substrate's orbitals.

Figure 5a shows the θ_i -dependent change in the intensities of the 4a₁ peak (●) and the 400-eV peak (○). Although the intensities of both peaks show a decreasing trend with increasing θ_i , the scatter of the data is rather large. This is because the 4a₁ peak and the low energy peak at 400 eV overlap significantly, and thus, the evaluated intensities of these peaks depends strongly on several possible fitting results (Figure 5b-d).³⁵ Thus, it is difficult to access the true θ_i -dependent change of the intensities for the 4a₁ state as well as the low energy state at 400 eV. On the other hand, the intensities of the 2e and high-lying hybrid peaks at 404 and 407 eV, respectively, can be uniquely determined, since these peaks are well separated from the neighboring peaks so that the evaluated peak intensities are almost independent of the different fitting results as shown in Figure 5b-d. In Figure 6a,b, we plotted the integrated intensities of the 2e and high-lying hybrid peaks as a function of θ_i . Clear

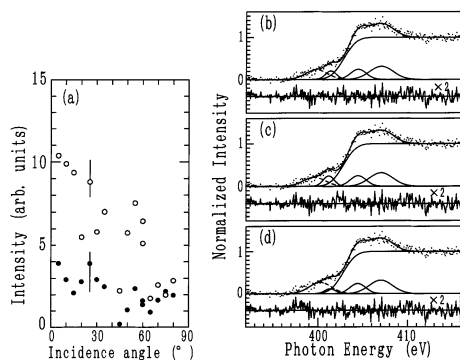


Figure 5. (a) The θ_i -dependent change in the intensities of the $4a_1$ peak (●) and the 400-eV peak (○). (b–d) Three different results of curve fitting analysis for the spectrum taken at $\theta_i = 25^\circ$. The standard deviations are (b) 2.332×10^{-2} (the best fit), (c) 2.339×10^{-2} , and (d) 2.343×10^{-2} . The deviations of the latter two results differ by less than 1% from that of the best fit. The residuals are shown at the lower part of Figure 5b–d.

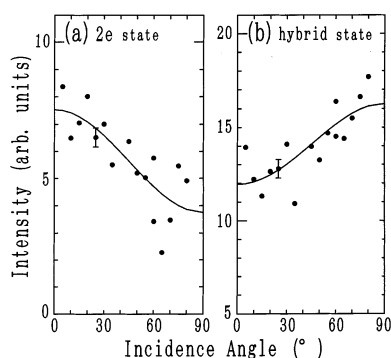


Figure 6. The θ_i dependence of the intensity of the peaks associated with (a) the 2e state and (b) the high-lying hybrid state. Filled circles are the observed data. The solid lines are the best fit to the data using eqs 2 and 3 for the 2e state ($\gamma = 33^\circ$) and hybrid state (41°), respectively.

increasing and decreasing trends are observed with increasing θ_i . In the following, we therefore focus our attention on the 2e and high-lying hybrid peaks.

The 2e peak exhibits a decreasing trend with increasing θ_i (Figure 6a). According to the dipole selection rules, the N 1s core-level electron is excited to the NH_3 2e orbital by the electric vector \mathbf{E} perpendicular to the C_{3v} axis of NH_3 .³⁶ On the $\text{ZnO}(10\bar{1}0)$ surface, it is considered that the C_{3v} axis of adsorbed NH_3 is oriented in the $[000\bar{1}]$ mirror plane, because the dangling bonds of the surface Zn and O atoms extend toward the $[000\bar{1}]$ and $[0001]$ direction, respectively, so that adatoms bonded to the surface Zn or O atoms should be in the $[000\bar{1}]$ mirror plane. In such a case, the 2e peak intensity I_{2e} is given by the following relation using the tilt angle γ and the incidence angle of light θ_i , both of which are measured from the surface normal:³⁶

$$I_{2e} \propto P \left[1 - \cos^2 \left(\frac{\pi}{2} - \theta_i \right) \cos^2 \gamma - \sin^2 \left(\frac{\pi}{2} - \theta_i \right) \sin^2 \gamma \right] + (1 - P) \quad (2)$$

where P is a degree of polarization and is estimated to be ~ 0.9 in the present study. Using the above relation, $\gamma = 33^\circ$ gives the best fit to the data in Figure 6a.

The peak associated with the high-lying hybrid states at 407 eV shows an increasing behavior with θ_i (Figure 6b). This means that the MO's with a different symmetry from the e symmetry should contribute to the 407-eV peak, i.e., the a_1 orbitals are

responsible for the observed θ_i dependence. The intensity of the peak with the a_1 symmetry I_{a_1} is expressed as follows:³⁶

$$I_{a_1} \propto P \left[\cos^2 \left(\frac{\pi}{2} - \theta_i \right) \cos^2 \gamma + \sin^2 \left(\frac{\pi}{2} - \theta_i \right) \sin^2 \gamma \right]. \quad (3)$$

The observed θ_i dependence of the 407-eV peak intensity is best fitted at $\gamma = 41^\circ$. Among the NH_3 MO's contributing to the high-lying hybrid states, the N $3p_z$ -, $4s$ -, and $4p_z$ -derived orbitals have the a_1 symmetry. However, the MO's with the e symmetry, such as the N $4p_{xy}$ -derived orbitals, also contribute to the peak at 407 eV, and thus, the observed θ_i dependence in Figure 6b could be somewhat modified from the expected θ_i dependence of the resonance which involves only the a_1 orbitals. Within the framework of the single-particle picture for the photoabsorption process, the transition probability of the N 1s electron to the MO's composed of the N $3p$, $4s$, and $4p$ orbitals decreases with increasing principal quantum number because of the decreasing overlap between the core and valence orbitals.³⁷ This implies that the modification of the θ_i -dependent change in the peak intensity by the N $4p_{xy}$ contribution should not be large.

It is noted that the low-energy structure at ~ 400 eV shows a decreasing trend with increasing θ_i (Figure 5a), although the data points are scattered and contain a relatively large uncertainty as discussed above. We have temporarily assigned this structure to the transition of the N 1s electron to the hybridized states between NH_3 $3a_1$, $4a_1$, 2e, etc., MO's and the substrate's orbitals. Although more detailed studies is requisite in order to reveal the origin of this peak, it is considered that the MO's with the e symmetry should contribute largely to the hybridized states, because the peak intensity decreases with increasing θ_i .

IV. Discussion

The NEXAFS measurements reveal that ammonia adsorbs on $\text{ZnO}(10\bar{1}0)$ with its C_{3v} molecular axis tilted by 33° – 41° from the surface normal along the $[000\bar{1}]$ azimuth. The experimentally determined tilt angle is in excellent agreement with the theoretically evaluated angle of 34° .⁵ This demonstrates that the NEXAFS technique, combined with curve-fitting analysis, is applicable for determination of the orientation of adsorbates which does not exhibit sharp resonances.

From the valence-band PES measurements, it is found that NH_3 chemisorbs on $\text{ZnO}(10\bar{1}0)$ through the N-localized $3a_1$ MO, i.e., the N atom is directly involved in the chemical bond formation with the surface. However, no information is available for the adsorption sites of NH_3 on $\text{ZnO}(10\bar{1}0)$ in the present study. As far as we know, the adsorption sites of NH_3 on $\text{ZnO}(10\bar{1}0)$ have not been directly proved experimentally. However, Solomon et al. have found from the PES measurements that both NH_3 and carbon monoxide (CO) adsorb at the same adsorption sites on $\text{ZnO}(10\bar{1}0)$,¹¹ and the CIS studies in the Zn $3p \rightarrow 4s$ transition region have revealed that the Zn $4s$ orbital is involved in the bonding interaction with CO.¹² These results imply that NH_3 is bound to the surface Zn atoms. Such an adsorption manner is reasonable since NH_3 is a strong Lewis base and should interact with the surface Lewis acid, i.e., the Zn cations on $\text{ZnO}(10\bar{1}0)$. Thus, adsorption of NH_3 on the Zn ion should proceed via an orbital hybridization between the N-localized $3a_1$ orbital of NH_3 and the unoccupied $4sp$ dangling bond orbital of the surface Zn ion, leading to the σ -type N–Zn chemical bond. Adsorption of NH_3 on the Zn site makes the chemical environment of the surface Zn atoms being more bulklike, since NH_3 substitutes for the missing ligand of the unsaturated surface Zn atoms. Thus, NH_3 adsorption should

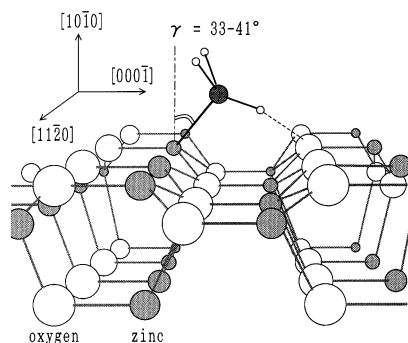


Figure 7. A schematic geometry of molecularly adsorbed NH_3 on the $\text{ZnO}(10\bar{1}0)$ surface. On the bases of the DF calculations by Casarin et al.,⁵ one of the three H atoms is assumed to be involved in hydrogen bonding with the surface O atom.

induce the attenuation of the surface states of the Zn 3d band, which is responsible for the observed narrowing of the Zn 3d peak upon adsorption.

Although it is highly probable that NH_3 is bonded to the surface Zn atoms, the O 2p dangling bond states at ~ 4 eV are affected by adsorption (Figure 2). The shift of the O 2p dangling bond states is considered to be due to the electrostatic interaction between the H atom of NH_3 and the surface O atom, i.e., the hydrogen bonding. Since adsorbed NH_3 is tilted away from the surface normal, one of the three H atoms lies so close to the surface O atom that the hydrogen bond is possible between H and O. Such an electrostatic interaction must perturb the spatial distribution of the O 2p dangling bond orbital, which is largely extended toward the vacuum on the NH_3 -free surface, when the H atom of NH_3 positions close to the surface O atom. This results in the observed shift of the O 2p dangling bond states to the higher binding energy side. Figure 7 shows an adsorption model of NH_3 on $\text{ZnO}(10\bar{1}0)$. The H atom should be hydrogen-bonded to the O atom in the Zn–O row next to the Zn–O row in which the N atom is bonded to the Zn atoms.

The formation of the hydrogen bond between ammonia and the metal oxide surfaces is also suggested for other adsorption systems. Recent DF cluster calculations by Nakajima and Doren⁴ have shown that NH_3 on the $\text{MgO}(001)$ surface is bound to the Mg cation via its N atom by the σ -type interaction and that adsorption is further stabilized by the electrostatic interaction between the H atom of NH_3 and the surface O atom. Although NH_3 adsorbs on the atomically flat $\text{MgO}(001)$ surface, the hydrogen bond formation results in tilted NH_3 .⁴ A similar effect of the hydrogen bond formation upon the tilted orientation of NH_3 is expected to be also operative for the $\text{NH}_3/\text{ZnO}(10\bar{1}0)$ system. When NH_3 adsorbs on the coordinately incomplete surface Zn atoms, the tilt angle between the Zn–N axis and the surface normal is expected to be 19° , which corresponds to the tetrahedral direction of the dangling bond of the surface Zn atoms on the unrelaxed surface. However, the experimentally observed and theoretically estimated tilt angles are 33° – 41° and 34° ,⁵ respectively. Such a large tilt angle should be a consequence of hydrogen bonding between NH_3 and the $\text{ZnO}(10\bar{1}0)$ surface. Therefore, adsorbed NH_3 is considered to be stabilized through the formation of the hydrogen bond even though an enlarged tilt of the Zn–N bond should destabilize the local structure of the substrate surface due to the enlarged strain energy.

A large inclination of adsorbed molecules compared with the tetrahedral direction of 19° is also found for CO adsorbed on $\text{ZnO}(10\bar{1}0)$. Angle-resolved PES study by Sayers et al. has revealed that the molecular axis of CO is tilted by $\sim 30^\circ$ relative

to the surface normal direction.^{38,39} The tilting of CO from the ideal angle of 19° is considered to arise from the electrostatic interaction between CO and the nearest oxide ion of the substrate surface.³⁸ Another possible mechanism is proposed that the tilted geometry serves to reduce the expected strong dipole–dipole repulsive interaction between adsorbed CO, since CO is still polarized after adsorbing on the surface.³⁹ Ammonia has a large dipole moment of 1.53 D in the gas phase,⁴⁰ and the adsorbed NH_3 molecule has the apparent dipole moment of 0.7 D with the negative end being directed toward the bulk side on $\text{ZnO}(10\bar{1}0)$.²⁷ This implies that a strong dipole–dipole repulsive interaction between NH_3 should be operative. Therefore, apart from the formation of the hydrogen bond between NH_3 and the $\text{ZnO}(10\bar{1}0)$ surface, the large inclination of NH_3 could also result from the suppression mechanism of the direct dipole–dipole interaction between adsorbed NH_3 . The contribution of this mechanism can be accessed by the coverage-dependent study by the NEXAFS spectroscopy.

Finally, we comment on the possible origin of the decomposition reaction of ammonia on the $\text{ZnO}(0001)$ surface¹⁰ on the bases of the results obtained from the present study. The present study shows that ammonia adsorbs molecularly on the nonpolar $\text{ZnO}(10\bar{1}0)$ surface at room temperature. Our recent PES study has indicated that the dissociated species are formed at 350 K.²⁷ On the other hand, decomposed species are already formed at 130 K on $\text{ZnO}(0001)$,¹⁰ indicating high reactivity of $\text{ZnO}(0001)$ toward the decomposed reaction of NH_3 . The N 1s core-level PE spectra (Figure 5 in ref 10) show that, although molecularly adsorbed ammonia is the main species on the surface at high NH_3 coverages, the decomposed species are dominant over chemisorbed NH_3 at low coverages. This suggests that there should exist particularly high active sites for the ammonia decomposition reaction on $\text{ZnO}(0001)$. Unlike the nonpolar $\text{ZnO}(10\bar{1}0)$ surface, which is one of the most stable low-index surfaces of single crystal ZnO, the polar $\text{ZnO}(0001)$ surface contains thermally etched hexagonal pits with a step height of ~ 6 Å with a relatively high density.⁴¹ These step sites often exhibit high reactivity because of the high densities of occupied and unoccupied dangling bonds.⁴² Therefore, although a detailed study is requisite to reveal the origin of high reactivity of $\text{ZnO}(0001)$ compared with the $(10\bar{1}0)$ surface, the hexagonal pits on the (0001) surface are the most plausible candidate for the ammonia-dissociation site.

V. Summary

The adsorption state of ammonia on the nonpolar $\text{ZnO}(10\bar{1}0)$ surface has been investigated utilizing core-level and valence-band PES. Ammonia adsorbs molecularly on the surface at room temperature through the N-localized $3a_1$ orbital. Since recent studies have proved that NH_3 adsorbs on the Zn atoms on $\text{ZnO}(10\bar{1}0)$, NH_3 adsorption should result in the Zn–N chemical bond formation. The orientation of NH_3 on $\text{ZnO}(10\bar{1}0)$ is determined by the polarization dependent NEXAFS measurements combined with curve-fitting analysis. Adsorbed NH_3 is found to be inclined in the $[0001]$ azimuth with the tilt angle of 33° – 41° relative to the surface normal. The observed tilt angle is larger than the expected tilt of 19° , which corresponds to the tetrahedral direction of the dangling bond of the surface Zn atoms on the unrelaxed surface. Hydrogen bonding between the H atom of NH_3 and the surface O atom, which is inferred from the adsorption-induced shift of the O 2p dangling bond states to the higher binding energy side, is considered to be responsible for the large tilt angle of NH_3 on $\text{ZnO}(10\bar{1}0)$.

Acknowledgment. The work associated with the NEXAFS measurements was supported by the Joint Studies Program (2000–2001) of the Institute for Molecular Science. The authors acknowledge the staff of the UVSOR facility, the Institute for Molecular Science, for their excellent support.

References and Notes

- (1) Bowker, M. *The Chemical Physics of Solid Surfaces*; King, D. A., Woodruff, D. P., Eds.; Elsevier: Amsterdam, 1993; Vol. 6, p 225.
- (2) Li, Y.; Armor, J. N. *Appl. Catal. B: Environ.* **1997**, *13*, 131.
- (3) Markovits, A.; Ahdjoudj, J.; Minot, C. *Surf. Sci.* **1996**, *365*, 649.
- (4) Nakajima, Y.; Doren, D. J. *J. Chem. Phys.* **1996**, *105*, 7753.
- (5) Casarin, M.; Maccato, C.; Vittadini, A. *Chem. Phys. Lett.* **1999**, *300*, 403.
- (6) Román, E. L.; de Segovia, J. L.; Kurtz, R. L.; Stockbauer, R.; Madey, T. E. *Surf. Sci.* **1992**, *273*, 40 and references therein.
- (7) Román, E.; de Segovia, J. L. *Surf. Sci.* **1991**, *251/252*, 742.
- (8) Ma, H.; Berthier, Y.; Marcus, P. *Appl. Surf. Sci.* **1999**, *153*, 40.
- (9) Siu, W. K.; Bartynski, R. A.; Hulbert, S. L. *J. Chem. Phys. B* **2000**, *113*, 10697.
- (10) Lin, J.; Jones, P. M.; Lowery, M. D.; Gay, R. R.; Cohen, S. L.; Solomon, E. I. *Inorg. Chem.* **1992**, *31*, 686.
- (11) Gay, R. R.; Nodine, M. H.; Henrich, V. E.; Zeiger, H. J.; Solomon, E. I. *J. Am. Chem. Soc.* **1980**, *102*, 6752.
- (12) Lin, J.; Jones, P.; Guckert, J.; Solomon, E. I. *J. Am. Chem. Soc.* **1991**, *113*, 8312.
- (13) Walsh, J. F.; Davis, R.; Murny, C. A.; Thornton, G.; Dhanak, V. R.; Prince, K. C. *Phys. Rev. B* **1993**, *48*, 14749.
- (14) Davis, R.; Walsh, J. F.; Murny, C. A.; Thornton, G.; Dhanak, V. R.; Prince, K. C. *Surf. Sci.* **1993**, *298*, L196.
- (15) Hövel, St.; Kolczewski, C.; Wühh, M.; Albers, J.; Weiss, K.; Staemmler, V.; Wöll, Ch. *J. Chem. Phys.* **2000**, *112*, 3909.
- (16) Gutiérrez Sosa, A.; Evans, T. M.; Parker, S. C.; Campbell, C. T.; Thornton, G. *J. Phys. Chem. B* **2001**, *105*, 3783.
- (17) Strongin, D.; Mowlem, J. *Surf. Sci.* **1991**, *247*, L209.
- (18) Jaeger, R.; Stöhr, J.; Kendelewicz, T. *Surf. Sci.* **1983**, *134*, 547.
- (19) Hasselström, J.; Föhlisch, A.; Karis, O.; Wassdahl, N.; Weinelt, M.; Nilsson, A.; Nyberg, M.; Petersson, L. G. M.; Stöhr, J. *J. Chem. Phys.* **1999**, *110*, 4880.
- (20) Benndorf, C.; Madey, T. E. *Surf. Sci.* **1983**, *135*, 164.
- (21) Mocuta, D.; Ahner, J.; Yates, J. T. *Surf. Sci.* **1997**, *383*, 299.
- (22) Booth, N. A.; Davis, R.; Toomes, R.; Woodruff, D. P.; Hirschnugl, C.; Schindler, K. M.; Schaff, O.; Fernandez, V.; Theobald, A.; Hofmann, Ph.; Lindsay, R.; Gießel, T.; Baumgärtel, P.; Bradshaw, A. M. *Surf. Sci.* **1997**, *387*, 152.
- (23) Rodriguez, J. A.; Jirsak, T.; Chaturvedi, S.; Kuhn, M. *Surf. Sci.* **1999**, *442*, 400.
- (24) Shikin, A. M.; Gorovikov, S. A.; Adamchuk, V. K.; Molodtsov, S. L.; Engelmann, P.; Laubschat, C. *J. Electron Spectrosc. Relat. Phenom.* **1999**, *105*, 85.
- (25) Outka, D. A.; Stöhr, J. *J. Chem. Phys.* **1988**, *88*, 3539.
- (26) Galtayries, A.; Laksono, E.; Siffre, J.-M.; Argile, C.; Marcus, P. *Surf. Interface Anal.* **2000**, *30*, 140 and references therein.
- (27) Ozawa, K.; Edamoto, K. *Surf. Rev. Lett.* **2002**, *9*, 717.
- (28) Equation 1 is derived from the model that the observed O 1s PE intensity I_{O1s} from the clean ZnO(1010) surface is given by the sum of the intensities from the (1010) planes, which decay exponentially with the distance from the surface.
- (29) Yeh, J. J.; Lindau, I. *Atom. Data Nucl. Data Table* **1985**, *32*, 1.
- (30) Seah, M. H.; Dench, W. A. *Surf. Interface Anal.* **1972**, *1*, 2.
- (31) The Zn-related parameters used for the calculation are as follows: $I_{N1s}/I_{Zn2p_{3/2}} = 2.30 \times 10^{-3}$, $\sigma_{Zn2p_{3/2}} = 0.260$ Mb, and $\lambda_{Zn2p_{3/2}} = 10$ Å.
- (32) Göpel, W.; Pollmann, J.; Ivanov, I.; Reihl, B. *Phys. Rev. B* **1982**, *26*, 3144.
- (33) Turner, D. W.; Baker, C.; Baker, A. D.; Brundle, C. R. *Molecular Photoelectron Spectroscopy*; Wiley-Interscience: London, 1970; p 356.
- (34) Schirmer, J.; Trofimov, A. B.; Randall, K. J.; Feldhaus, J.; Bradshaw, A. M.; Ma, Y.; Chen, C. T.; Sette, F. *Phys. Rev. A* **1993**, *47*, 1136.
- (35) In Figures 5b–d, we show how the intensities of the 4a₁ peak and the 400-eV peak cannot be uniquely determined. Figure 5b shows the best fit to the spectrum taken at $\theta_i = 25^\circ$ with the standard deviation of 2.332×10^{-2} . The other two results (Figures 5c and 5d) are also plausible since their standard deviations differ by less than 1% from that of the best fit. However, integrated intensities of the 4a₁ and 400-eV peaks depends significantly on the fitting results; the intensity of the 4a₁ peak changes from 2.2 to 4.6, while that of the 400-eV peak from 10.2 to 7.9. Vertical bars in Figure 5a show these variations. Such a large uncertainty for the intensities of the 4a₁ and 400-eV peaks is obtained in the spectra especially taken at $\theta_i \geq 20^\circ$, where the 4a₁ peaks is no more observed clearly.
- (36) Stöhr, J.; Outka, D. A. *Phys. Rev. B* **1987**, *36*, 7891.
- (37) Björneholm, O.; Nilsson, A.; Zdansky, E. O. F.; Sandell, A.; Tillborg, H.; Andersen, J. N.; Mårtensson, N. *Phys. Rev. B* **1993**, *47*, 2308.
- (38) Sayers, M. J.; McClellan, M. R.; Gay, R. R.; Solomon, E. I.; McFeely, F. R. *Chem. Phys. Lett.* **1980**, *75*, 575.
- (39) D'Amico, K. L.; McClellan, M. R.; Sayers, M. J.; Gay, R. R.; McFeely, F. R.; Solomon, E. I. *J. Vac. Sci. Technol.* **1980**, *17*, 1080.
- (40) Halkier, A.; Taylor, P. R. *Chem. Phys. Lett.* **1998**, *285*, 133.
- (41) Möller, P. J.; Komolov, S. A.; Lazneva, E. F. *Surf. Sci.* **1994**, *307*–*309*, 1177.
- (42) Parker, T. M.; Condon, N. G.; Lindsay, R.; Leible, F. M.; Thornton, G. *Surf. Sci.* **1998**, *415*, L1046.